Au_3SnCuP_{10} and Au_3SnP_7: Preparation and Crystal Structures of Au_3Sn Heterocluster Polyphosphides

Stefan Lange and Tom Nilges

Institut für Anorganische und Analytische Chemie, Westfälische Wilhelms-Universität Münster, Corrensstraße 30, D-48149 Münster, Germany

Reprint requests to Dr. T. Nilges. Fax: +49 251 83 36002. E-mail: nilges@uni-muenster.de

Z. Naturforsch. **61b,** 871 – 881 (2006); received March 3, 2006

Dedicated to Professor Wolfgang Jeitschko on the occasion of his 70th birthday

The formation of Au_3Sn heteroclusters completes the homologous series of M_3Sn clusters observed for transition metal main-group polyphosphides. Au_3SnCuP_{10} is cubic, space group $F43m$ (No. 216) with lattice parameter $a = 10.3953(5)$ Å. The structure refinement yielded $R1 = 0.0353$ and $wR2 = 0.0726$ for 154 F^2 values and 13 variables. Disordered Au_3Sn heteroclusters occupy all octahedral, and adamantane like P_{10} cages one half of the tetrahedral voids of a face-centred cubic (fcc) arrangement of copper. Ordered and orientationally disordered Au_3Sn heteroclusters have been observed for Au_3SnP_7, embedded in a $^1_\infty[P_7]$ polyphosphide unit formed by six-membered phosphorus rings in chair conformation which are linked by a P-bridge. Au_3SnP_7 is monoclinic, space group $P2_1/m$ (No. 11) with lattice parameters of $a = 6.219(2)$, $b = 10.836(2)$, $c = 6.318(2)$ Å, $\beta = 108.65(2)^\circ$, $V = 403.4(2)$ Å^3, $R1 = 0.0412$ and $wR2 = 0.0745$, 1261 F^2 values and 56 variables. Au_3SnP_7 with disordered Au_3Sn clusters has slightly larger lattice parameters of $a = 6.343(3)$, $b = 10.955(3)$, $c = 6.372(3)$ Å, $\beta = 108.63(2)^\circ$, $V = 419.6(2)$ Å^3, $R1 = 0.0324$ and $wR2 = 0.0691$, 1131 F^2 values and 58 variables.

Key words: Polyphosphides, Heterocluster, Structure Determination

Introduction

Elemental phosphorus [1], phosphides and polyphosphides [2, 3] are showing extraordinary structural chemistry in a plethora of materials, interesting physical properties and a large range of chemical compositions. Two of the most exciting fields are rare earth/transition metal phosphides predominantly examined in the groups of Jeitschko, Mewis, Kuz'ma or Guérin [3, 4] or the main group phosphides and polyphosphides with pioneer work done in the groups of von Schnering [2] or Baudler [5].

We have focused our interest on phosphide materials with cations like $M = Li^+$, Cu^+ and Ag^+ showing a high potential for electrochemical applications. Recently, binary phosphides like Zn_3P_2 [6] or Cu_3P [7] were found to be potential candidates for anode materials in rechargeable batteries. The number of binary phosphides and polyphosphides of the mentioned cations decreases from $M = Li^+$ ($M_3P \ldots MP_{15}$) [3] over Cu^+ (M_3P, MP_2, M_2P_7) [8–10] to Ag^+ (MP_2, M_3P_{11}) [9–11]. The same general trend can be observed for ternary phosphides. In the case of ternary polyphosphides only a very limited number of compounds has been characterised so far, containing lithium or group 11 metals. $LiCu_2P_2$ [12] and $Li_7Cu_5P_8$ [13] are two examples with a very high content of the expected ions. Only two compounds, Cu_3SnCuP_{10} [14, 15] and Ag_3SnP_7 [16], have been described in literature featuring M_3Sn heteroclusters. Very recently we were able to prepare Ag_3SnCuP_{10} [17], the silver homologue of Cu_3SnCuP_{10}. Using a combined strategy of diffraction methods, solid state NMR and Mössbauer spectroscopy an orientational disorder of the M_3Sn clusters was identified as the only realized disorder type in those materials. Surprisingly, the heavier M_3Sn homologue in this row, Au_3Sn, is not known.

The electronic situation of the 32 electron M_3Sn heteroclusters has been described for Ag_3SnP_7 and Cu_3SnCuP_{10} [16, 18]. Eight electrons contribute to the bonding between the cluster atoms with attractive interactions of the tin s orbitals and M d orbitals consistent with a 3 centre-2 electron bond system. Interaction

of tin p orbitals and silver s and p orbitals are responsible for the covalent bonding to the phosphorus environment. Both compounds are semiconductors with band gaps of 0.2 (Ag_3SnP_7) and 1.2 eV (Cu_3SnCuP_{10}) [15].

Herein we report on the preparation and structural features of Au_3SnCuP_{10} and Au_3SnP_7, two new polyphosphides containing the heterocluster Au_3Sn.

Results and Discussion

Au_3SnCuP_{10}

The preparation of Au_3SnCuP_{10} using a conventional high temperature synthesis from the elements (method 1) led to the formation of significant amounts

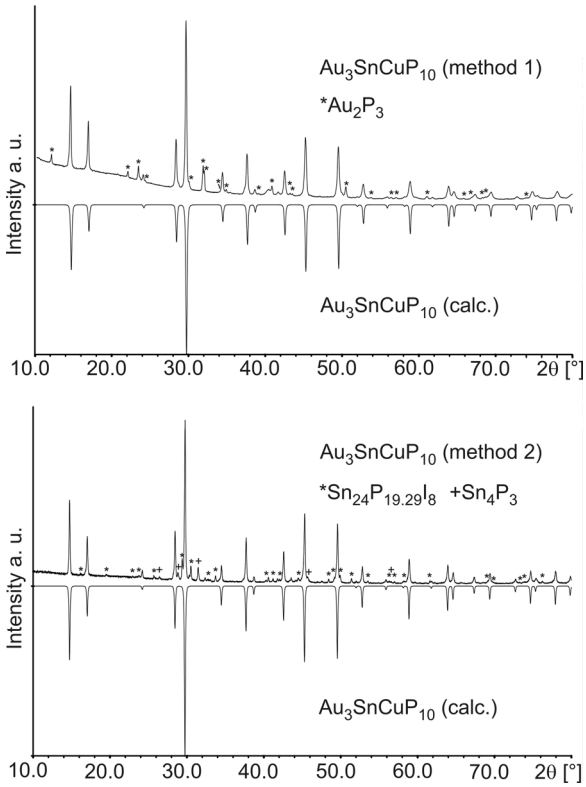

Fig. 1. X-ray powder diffractograms of Au_3SnCuP_{10} bulk material prepared *via* two different synthetic routes. Method 1 represents the common synthesis from stoichiometric amounts of starting materials and method 2 the reaction of the elements with additional SnI_4. Refined lattice parameters are $a = 10.3953(5)$ Å for method 1 and $a = 10.396(2)$ Å for method 2 rejecting the reflections of the side products Au_2P_3 [19], $Sn_{24}P_{19.29}I_8$ [20] and Sn_4P_3 [21], respectively. Those parameters are in good agreement with the value derived from single crystal data $a = 10.367(1)$ Å. Calculated diffractograms based on the single crystal data are drawn for comparison.

Table 1. Results from semiquantitative EDX analyses. Values are averaged from three to five independent measurements and are given in at.%. Estimated standard deviations in parentheses.

	Au	Sn	Cu	P
Au_3SnCuP_{10}:				
Calculated	20.0	6.67	6.67	66.67
Single crystal det.	16(2)	7(2)	11(2)	67(2)
Bulk	18(2)	9(2)	7(2)	66(2)
Au_3SnP_7:				
Calculated	27.27	9.09		63.63
Crystal 1	27(2)	11(2)		62(2)
Crystal 2	27(2)	10(2)		63(2)

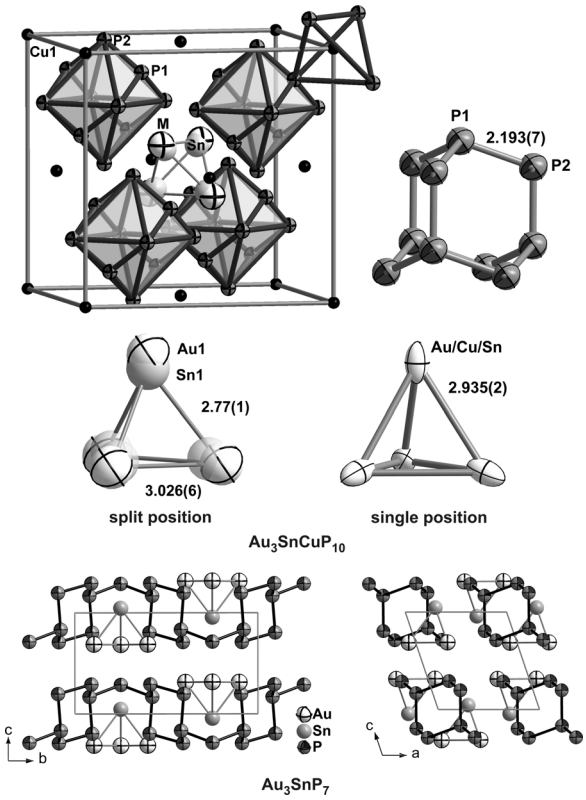

Fig. 2. Crystal structures of Au_3SnCuP_{10} (top) and Au_3SnP_7 (bottom). One CuP_4 coordination polyhedron and one disordered Au_3Sn heterocluster, localized around every octahedral void of the *fcc* type copper arrangement, are drawn. In the case of cubic Au_3SnCuP_{10} four adamantane-like P_{10} cages are centering half of the tetrahedral voids of the *fcc* cell. Au_3Sn clusters embedded in a $^1_\infty[P_7]$ polyphosphide unit formed by six-membered phosphorus rings and one linking P atom in 1,4 position are observed for Au_3SnP_7. Unit cells (dark grey lines) are drawn.

of Au_2P_3 [19] and further side products beside the expected polyphosphide (Fig. 1). The synthesis strategy could not be optimized by a variation of temperature or

Table 2. Crystallographic data for Au_3SnCuP_{10} and Au_3SnP_7 at 293 K.

	Refinement 1	Refinement 2	Crystal 1	Crystal 2
Empirical formula	Au_3CuSnP_{10}	Au_3CuSnP_{10}	Au_3SnP_7	Au_3SnP_7
refined formula	$Au_{2.43}CuSn_{0.90}P_{10}$	$Au_{2.41}Cu_{1.59}SnP_{10}$	Au_3SnP_7	$Au_{2.99(3)}Sn_{1.00(3)}P_7$
M [g mole^{-1}]	958.9	1003.6	926.4	926.4
Crystal system	cubic	cubic	monoclinic	monoclinic
Space group	$F\bar{4}3m$ (No. 216)		$P2_1/m$ (no. 11)	$P2_1/m$ (no. 11)
Lattice parameters [Å,°]	$a = 10.3953(5)$[a]	$a = 10.3953(5)$[a]	$a = 6.219(2)$ $b = 10.836(2)$ $c = 6.318(2)$ $\beta = 108.65(2)$	$a = 6.343(3)$[a] $b = 10.955(3)$ $c = 6.372(3)$ $\beta = 108.63(2)$
Cell volume [Å^3]	1123.34(9)		403.4(2)	419.6(3)
Z	4		2	
ρ_{X-ray} [g cm^{-3}]	5.67	5.93	7.62	7.33
Absorption correction	numerical			
μ [mm^{-1}]	36.8	38.9	58.7	56.5
Min/max transmission	0.130/0.262		0.088/0.177	0.046/0.101
$F(000)$	1664	1746	784	783
Crystal size [mm^3]	$0.08 \times 0.08 \times 0.06$		$0.05 \times 0.04 \times 0.04$	$0.04 \times 0.04 \times 0.03$
Diffractometer	CAD 4		IPDSII	
Radiation	Mo-K$_\alpha$			
Wavelength [Å]	0.71073			
Monochromator	graphite			
θ Max. [°]	31.0		30.41	31.94
No of reflections	2039		4184	4582
No. of independent reflections	154		1261	1131
Reflections $I > 3\sigma(I)$	129		871	787
No. of parameters	15	13	56	58
Refinement program	Jana2000 [50]			
R_{int}	0.208		0.0830	0.0390
$R1(I > 3\sigma(I))$	0.0349	0.0353	0.0412	0.0324
$wR2(I > 3\sigma(I))$	0.0701	0.0726	0.0745	0.0691
$R1$ (all)	0.0474	0.0484	0.0685	0.0526
$wR2$ (all) = for all reflexes	0.0737	0.0767	0.0795	0.0716
GoF	1.24	1.28	1.30	1.31
Flack parameter	0.02(6)	0.01(7)		
Max./min. residual electron density [e Å^{-3}]	2.00/−4.47	2.09/−1.11	3.26/−2.96	1.74/−3.48

[a] Lattice parameters from powder data.

annealing time. Multiple homogenisation and annealing steps did also not completely reduce the amount of side products in relation to Au_3SnCuP_{10}. Applying a modified strategy (method 2) by adding additional SnI_4 acting as a mineralization agent to the starting materials improved the synthesis results significantly. This method was used by Shatruk *et al.* for the synthesis of Ag_3SnP_7 [16] and could be successfully transferred to the preparation of Ag_3SnCuP_{10} [17]. The formation of Au_2P_3 was not observed any more but the introduction of SnI_4 led to the formation of small amounts of chathrate type $Sn_{24}P_{19.29}I_8$ [20] and Sn_4P_3 [21]. Crystalline gold or copper rich side products could not be detected. Nevertheless, significantly faster reaction times and an improvement of the overall crystallinity of the polyphosphide, observable for instance from the reduction of the reflection half width (width of the strongest reflection (2 2 2): 0.185° method 1 and 0.155° method 2) from X-ray phase analysis (Fig. 1), substantiates this finding. A possible disorder phenomenon which can also be responsible for such a half width increase will be discussed below in the structure description section. Refinements of the X-ray powder diffractograms of cubic Au_3SnCuP_{10}, prepared *via* both methods, led to exactly the same lattice parameters within one times the standard deviation of $a = 10.3953(5)$ Å for method 1 and $a = 10.396(2)$ Å for method 2. This result can be interpreted in such a way that a phase width with drastic effects on the lattice parameters is not present in this case. A comparison of powder diffractograms calculated from the single crystal data of Cu_3SnCuP_{10} ($a = 10.252(1)$ Å) and Ag_3SnCuP_{10} ($a = 10.503(1)$ Å) [17] pointed towards an isostructural crystallisation for Au_3SnCuP_{10}. Semi-

Table 3. Atomic coordinates and isotropic displacement parameters [Å^2] and site occupancy factors (sof) for Au_3SnCuP_{10} and Au_3SnP_7.

Atom	Wyckhoff	x	y	z	U_{iso}	sof
Au_3SnCuP_{10} refinement 1						
Cu1	4a	0	0	0	0.001(1)	1
Au2	16e	0.6029(4)	x	x	0.0175(6)	0.61(6)
Sn2	16e	0.585(2)	x	x	0.006(6)	0.22(9)
P1	16e	0.1283(4)	x	x	0.010(1)	1
P2	24g	1/4	0.0063(8)	1/4	0.016(2)	1
Au_3SnCuP_{10} refinement 2						
Cu1	4a	0	0	0	0.011(2)	0.89(1)
Au1	4a	0	0	0	0.011	0.11
Au2	16e	0.5998(1)	x	x	0.0208(3)	0.57(3)
Cu2	16e	0.5998	x	x	0.0208	0.18(3)
Sn2	16e	0.5998	x	x	0.0208	0.25
P1	16e	0.1279(4)	x	x	0.008(2)	1
P2	24g	1/4	0.0066(8)	1/4	0.012(2)	1
Au_3SnP_7 crystal 1						
Au1	2e	0.9302(1)	1/4	0.6844(2)	0.0136(3)	1
Au2	4f	0.31398(9)	0.10306(7)	0.6876(1)	0.0155(2)	1
Sn	2e	0.3100(2)	1/4	0.0446(3)	0.0115(4)	1
P1	4f	0.8342(6)	0.0785(4)	0.1671(7)	0.013(1)	1
P2	4f	0.2813(5)	−0.0934(4)	0.1967(7)	0.012(1)	1
P3	4f	0.1996(6)	0.0889(4)	0.2908(7)	0.011(1)	1
P4	2e	0.7335(8)	1/4	0.286(1)	0.011(2)	1
Au_3SnP_7 crystal 2						
Au1a	2e	0.9358(2)	1/4	0.6857(2)	0.0156(4)	0.62(1)
Sn1a	2e	0.9358	1/4	0.6857	0.0156	0.38
Au2	4f	0.3135(1)	0.10316(6)	0.6870(1)	0.0176(2)	1
Au1b	2e	0.3132(2)	1/4	0.0572(2)	0.0168(4)	0.37(1)
Sn1b	2e	0.3132	1/4	0.0572	0.0168	0.63
P1	4f	0.8340(6)	0.0783(3)	0.1662(7)	0.013(1)	1
P2	4f	0.2849(6)	−0.0909(3)	0.1966(6)	0.014(1)	1
P3	4f	0.1988(6)	0.0898(3)	0.2885(7)	0.014(1)	1
P4	2e	0.7266(8)	1/4	0.2797(9)	0.013(2)	1

quantitative EDX analyses of bulk material have substantiated the postulated composition of the polyphosphide (see Table 1). Values in at% of Au 18(2), Sn 9(2), Cu 7(2) and P 66(2) are in good agreement with the theoretical values of Au (20), Sn (6.67), Cu (6.67) and P (66.67) for Au_3SnCuP_{10}.

A single crystal structure determination was performed for Au_3SnCuP_{10} prepared by method 2. Au_3SnCuP_{10} crystallises isostructurally to the lighter homologues Cu_3SnCuP_{10} [15] and Ag_3SnCuP_{10} [17] in space group $F\bar{4}3m$. Characteristic structural features of this fascinating class of materials are M_3Sn heteroclusters and adamantane type P_{10} cages. Fig. 2, top part, gives an overview on the crystal structure and the structural units realized for the cubic polyphosphide. The heteroclusters are centered around the octahedral and the P_{10} cages on one half of the tetrahedral voids of a fcc arrangement of copper ions.

It has been shown for Cu_3SnCuP_{10} and Ag_3SnCuP_{10} earlier on that an orientational disorder of the M_3Sn heterocluster relative to the P_{10} cages occurs, and a substitutional disorder leading to $M_{3-x}Sn_x$ or $M_{3-y}Cu_ySn$ clusters is not present. Transferring those results to the gold polyphosphide a structural model with one Au (occupancy factor 0.75) and Sn (occ. 0.25) position leading to orientationally disordered Au_3Sn heteroclusters around the octahedral voids of the copper fcc cell was chosen as a starting model (refinement 1 in Table 2) for the structure refinement. Two very closely neighboured Au and Sn positions d(Au-Sn) = 0.31(2) Å were found to lead to correlations between the displacement parameters and occupancy factors. Therefore a restricted refinement (refinement 2) with equivalent positional and displacement parameters was applied to avoid these correlations. Crystallographic data and atomic coordinates for both refinements can be found in Tables 2 to 4. Independent from the way of refinement the overall scattering power for the 16e cluster atoms was not high enough to fulfil a complete occupancy of one Au_3Sn cluster per octahedral void. Two scenarios can be discussed, one is a cluster deficiency

Table 4. Anisotropic displacement parameters [Å^2] for Au_3SnCuP_{10} and Au_3SnP_7.

Atom	U_{11}	U_{22}	U_{33}	U_{12}	U_{13}	U_{23}
Au_3SnCuP_{10} refinement 1						
Au1	0.018(1)	U_{11}	U_{11}	0.002(2)	U_{12}	U_{12}
P1	0.010(2)	U_{11}	U_{11}	−0.0009(2)	$-U_{12}$	$-U_{12}$
P2	0.015(2)	0.017(4)	U_{11}	0	−0.002(3)	0
Au_3SnCuP_{10} refinement 2						
Au2	0.0199(6)	U_{11}	U_{11}	0.0076(7)	U_{12}	U_{12}
Sn2	0.0199	U_{11}	U_{11}	0.0076	U_{12}	U_{12}
Cu2	0.0199	U_{11}	U_{11}	0.0076	U_{12}	U_{12}
P1	0.008(3)	U_{11}	U_{11}	−0.002(2)	$-U_{12}$	$-U_{12}$
P2	0.012(2)	0.013(4)	U_{11}	0	−0.002(3)	0
Au_3SnP_7 crystal 1						
Au1	0.0121(4)	0.0138(5)	0.0145(4)	0	0.0038(3)	0
Au2	0.0107(3)	0.0211(4)	0.0140(3)	0.0006(3)	0.0032(2)	−0.0008(3)
Sn	0.0092(6)	0.0105(8)	0.0143(7)	0	0.0033(5)	0
P1	0.010(2)	0.016(2)	0.014(2)	0.001(2)	0.006(1)	0.001(2)
P2	0.009(2)	0.013(2)	0.013(2)	0.001(1)	0.002(1)	−0.001(2)
P3	0.008(1)	0.010(2)	0.012(2)	−0.001(1)	0.001(1)	−0.001(2)
P4	0.012(2)	0.009(3)	0.015(3)	0	0.006(2)	0
Au_3SnP_7 crystal 2						
Au1a	0.0220(6)	0.0120(5)	0.0162(6)	0	0.0108(4)	0
Sn1a	0.0220	0.0120	0.0162	0	0.0108	0
Au2	0.0173(3)	0.0203(3)	0.0180(3)	0.0009(2)	0.0095(2)	−0.0006(3)
Au1b	0.0168(6)	0.0123(6)	0.0242(8)	0	0.0106(5)	0
Sn1b	0.0168	0.0123	0.0242	0	0.0106	0
P1	0.014(2)	0.011(2)	0.016(2)	0.001(1)	0.007(1)	−0.001(1)
P2	0.016(2)	0.013(2)	0.016(2)	0.001(1)	0.009(1)	0.001(2)
P3	0.018(2)	0.011(2)	0.017(2)	0.0000(13)	0.0096(13)	−0.001(2)

and the second an $Au_{3-x}Cu_xSn$ heterocluster instead of an Au_3Sn one. A third option, the formation of tin rich heteroclusters has not been taken into account in accordance with the structural properties of the lighter homologues but should and will be addressed in further experiments. Compositions of approx. $Au_{2.4(2)}Sn_{0.9(2)}$ (refinement 1, split positions for Au/Sn) or $Au_{2.3(1)}Cu_{0.7(1)}Sn$ (refinement 2, restricted model with one Sn per cluster) were observed instead of Au_3Sn for the cluster positions. Also a mixed Cu/Au occupancy of the copper position was checked by a mixed Cu/Au refinement of the 4*a* position leading to 89(1)/11(1)% occupancy. In this case an alternate refinement of the occupancy factors of either the cluster positions or the copper/gold position had to be used. On comparing both refinements and taking the semiquantitative analyses of the single crystal into account (Table 1) the second refinement with a non-deficient but substitutionally disordered $Au_{2.3}Cu_{0.7}Sn$ heterocluster must be preferred. A refined composition of $(Au_{2.3}Cu_{0.7}Sn)Au_{0.11}Cu_{0.89}P_{10}$ (in at %: Ag (16.1) Cu (10.5), *Sn* (6.67) *P* (66.67)) is in reasonably good agreement with Au 16(2), Cu 11(2), Sn 7(2), P 67(2) derived from EDX analyses for the present crystal.

On the other hand it has to be stated, that this result should not be over interpreted due to the overall quality of the crystal. Nevertheless, a calculated powder diffractogram based on the results from structure determination shows a very good fit to the measured ones for bulk samples of Au_3SnCuP_{10} (Fig. 1). Therefore a certain substitutional $Au_{3-x}Cu_xSn$ disorder seems at least possible. Further investigations like solid state NMR spectroscopy and Mössbauer spectroscopy are planned to verify this assumption. During the ongoing discussion we will use the term Au_3SnCuP_{10} instead of $Au_{3-x}SnCu_{1+x}P_{10}$ never forgetting the uncertainties in the composition between EDX and X-ray data.

The cell volume of Au_3SnCuP_{10} (V = 1123.34(9) Å^3) is located between the copper (V = 1077.6(1) Å^3) and silver compound (V = 1158.5(1) Å^3) [17]. This effect which appears to be a volume anomaly on the first glance is a common effect found for several other more or less covalent or intermetallic compounds and is related to the effective radii and the volume requirements of the atoms. Focussing for instance on the metallic radii according to Pauling [22] silver ($r_{\text{met.}}(\text{Ag}) = 1.442$ Å, $CN = 12$; $r_{\text{met.}}(\text{Ag}) = 1.339$ Å, $CN(1)$) is slightly big-

ger than gold ($r_{\text{met.}}(\text{Au}) = 1.439$ Å, $CN = 12$; $r_{\text{met.}}(\text{Au}) = 1.336$ Å, $CN(1)$). A more drastic difference of 6% was observed for in the covalent radii of Ag (1.33 Å) compared with Au (1.25 Å) in [bis(trimesityl-phosphine)silver(I)]- and [bis(trimesitylphosphine)gold(I)] tetrafluoroborates [23]. Relativistic effects [24, 25] in the case of gold are also playing a dominant role and are responsible for a strong bonding interaction within the cluster. Jeitschko *et al.* have shown that the same relation is present in the covalent $HgPbP_{14}$ type polyphosphides $CdSnP_{14}$ ($V = 1357$ Å^3) [26] and $HgSnP_{14}$ ($V = 1341$ Å^3) [27] in going from Cd^{2+} to Hg^{2+}. Switching to the Ag/Au pair one can observe those volume relations for isotypic compounds in different coordination geometries and oxidation states like AgCN ($CN = 2$, $V_{\text{formula unit}} = 54.6$ Å^3) and AuCN ($CN = 2$, $V_{\text{formula unit}} = 50.9$ Å^3) [28] or Ag_2O_3 ($CN = 4$, $V = 494.6$ Å^3) [29] and Au_2O_3 ($CN = 4$, $V = 517.9$ Å^3) [30]. Several examples can also be found for intermetallics *e.g.* Ag_9In_4 ($CN = 12$, $V = 976.8$ Å^3) and Au_9In_4 ($CN = 12$, $V = 949.6$ Å^3) [31] or Ag_5Sr ($CN = 12$, $V = 127.8$ Å^3) [32] and Au_5Sr ($CN = 12$, $V = 126.6$ Å^3) [33].

The P-P bond distance of 2.193(7) Å is located within the expected range of 2.14 to 2.24 Å reported for other polyphosphide molecules like $P_7{}^{3-}$ in $Cs_3P_7 \cdot 3\ NH_3$ [34] or $[P_{11}]^{3-}$ in $Cs_3P_{11} \cdot 3\ NH_3$ [35]. An influence of the different M_3Sn heteroclusters on the bond lengths and bond angles of the P_{10} cages is not pronounced. Distances of 2.1789(6) and 2.192(2) Å have been found for Cu_3SnCuP_{10} and Ag_3SnCuP_{10}, respectively. The bond angles within the cages of all M_3SnCuP_{10} compounds vary in a very small range from 109.2 to 110.0°.

A discussion of heterocluster distances and M-P distances is not meaningful due to the uncertainties of the averaged values based on the mixed occupancies.

Au_3SnP_7

Following the same thermodynamically controlled synthesis strategy, starting from stoichiometric mixtures of the elements as used for Au_3SnCuP_{10}, the final product was only formed in rather small quantities. Au_2P_3, white phosphorus and binary intermetallic compounds of gold and tin like $AuSn_4$ [36] were observed instead. Adding a very small amount of SnI_4 to the starting materials did significantly reduce the amount of binary phases and Au_3SnP_7 was formed in very good yields (Fig. 3). Unfortunately, a small content of binary phases could not be reduced by multiple annealing steps or variations of the preparation conditions. Neglecting those reflections lattice parameters of $a = 6.343(3)$, $b = 10.955(3)$, $c = 6.372(3)$ Å, $\beta = 108.63(2)°$ and $V = 419.6(3)$ Å^3 were observed for Au_3SnP_7. A quite similar powder pattern compared with Ag_3SnP_7 implies an isotypic structure for both materials. Surprisingly, the clathrate type $Sn_{24}P_{19.29}I_8$ did not appear during the preparation process.

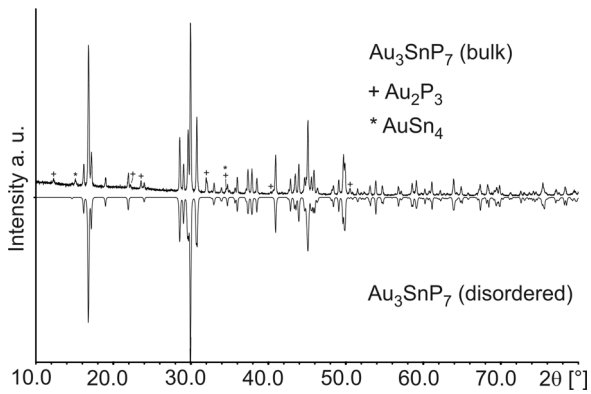

Fig. 3. X-ray powder diffractogram of Au_3SnP_7 bulk material (top). Refined lattice parameters of $a = 6.343(3)$, $b = 10.955(3)$, $c = 6.372(3)$ Å, $\beta = 108.63(2)°$, $V = 419.6(2)$ Å^3 have been observed rejecting the reflections of Au_2P_3 (+) [19] and $AuSn_4$ (*) [36]. Those parameters are in good agreement with the values derived from single crystal data $a = 6.329(2)$, $b = 10.944(4)$, $c = 6.364(2)$ Å, $\beta = 108.85(3)$. A calculated diffractogram based on the data of the disordered Au_3SnP_7 structure model (crystal 2) is drawn for comparison.

Semiquantitative analyses of multiple crystals separated from the bulk material and analyses of the single crystals used for structure determinations proved the overall composition of Au_3SnP_7 (see Table 1) within the accuracy of the applied method.

Intensity data of a single crystal were collected on a Stoe IPDS II system. The space group $P2_1/m$ was derived from systematic extinctions and a structural model related to Ag_3SnP_7 was used for the structure refinements. Convergence was achieved quickly and reasonably good R values pointed towards an isotypic structure for Au_3SnP_7 (see Table 1). Distorted tetrahedral Au_3Sn heteroclusters embedded in ${}^1_\infty[P_7]$ units are characteristic features of the polyphosphide (Fig. 2, bottom part). In order to verify the possibility of an Au/Sn disorder or a phase width lead-

ing to $Au_{3-x}Sn_{1+x}$ clusters, the occupancy factors of all cation positions were checked but neither the Sn nor the Au occupancy factors were significantly different from 1. Therefore a deviation of the lattice parameters ($a = 6.219(2)$, $b = 10.836(2)$, $c = 6.318(2)$ Å, $\beta = 108.65(2)^\circ$, $V = 403.4(2)$ Å^3), derived from the single crystal structure determination of crystal 1, compared with the results from X-ray powder phase analysis ($V = 419.6$ Å^3) were quite unsatisfactory. We decided to repeat the structure determination with additional crystals in order to find an explanation for the different results. A second crystal isolated from the same sample (crystal 2) showed increased lattice parameters, close to the ones found from phase analysis ($a = 6.325(2)$, $b = 10.935(3)$, $c = 6.358(2)$ Å; $\beta = 108.8(1)^\circ$ and $V = 416.2(2)$ Å^3). A refinement based on a structure model of crystal 1 converged well, but also left some unexpected peaks and holes around the 2*e* positions (Au1 and Sn). Applying a mixed Au and Sn distribution for both positions and performing a free refinement of the occupancy factors, restricted only to a full overall occupancy, led to a significant improvement of the structure model. With a 62(1)/38(1)% and 37(1)/63(1)% distribution of Au/Sn on the 2*e* positions a composition of $Au_{2.99(3)}Sn_{1.00(3)}P_{10}$ was observed in perfect agreement to the quantitative analysis. As a consequence from the structure determination result of crystal 2 it must be concluded that an orientational disorder of Au_3Sn heteroclusters can also be observed for Au_3SnP_7.

In combination with the results from phase analysis of bulk material it is obvious that the ordering process during the preparation is very slow and only a small quantity of crystals had reached the ordered state. Attempts to accelerate the ordering by changing the annealing temperature were not successful.

Focussing on the crystallographic data of the M_3SnP_7 compounds M = Ag, Au the same trend in the cell volumes can be found as reported for M_3SnCuP_{10}. The cell volumes of ordered ($V = 403.4(2)$ Å^3) or disordered Au_3SnP_7 ($V = 419.6(3)$ Å^3) are smaller compared with Ag_3SnP_7 ($V = 436.1$ Å^3) in good agreement with the trend found for the M_3SnCuP_{10} compounds.

The Au_3Sn heterocluster can be described as a distorted butterfly type tetrahedron with one elongated edge (see Fig. 4). Bond distances are d(Au-Au) = 2.864(1); d(Au-Sn) = 2.705(2) and 2.768(2) Å, in good agreement with distances reported for other Au/Sn clusters. Examples are $Rb_4Au_7Sn_2$ [37],

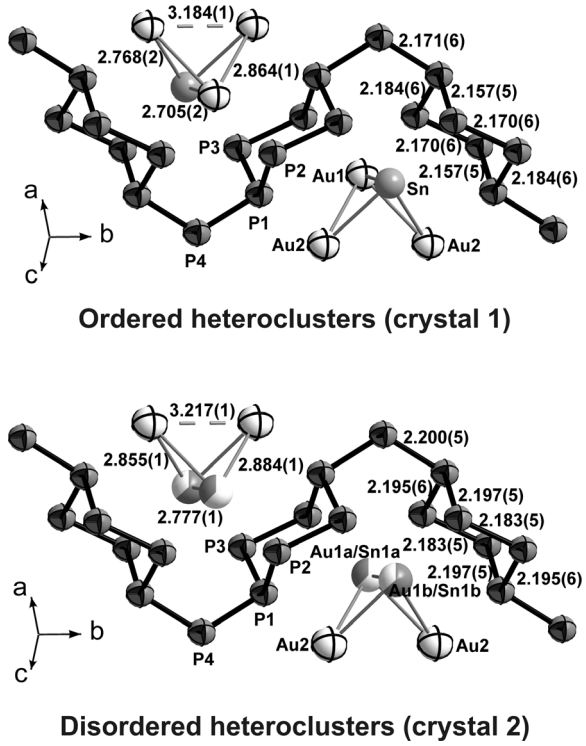

Fig. 4. Comparison of the $\frac{1}{\infty}[P_7]$ polyphosphide units of an ordered (crystal 1) and a disordered (crystal 2) Au_3Sn heterocluster arrangement in Au_3SnP_7. Differences in the grade of disorder have an averaging influence on the bond distance distribution within the six-membered polyphosphide rings. Distances in Å and displacement parameters at 90% probability.

KAu_4Sn_2 [38], $AuSn_2$ [39] and Au$M$$Sn_2$ (M = Cu, Ni) [40] with bond distances in the range of d(Au-Au) = 2.75 – 3.02 Å and d(Au-Sn) = 2.60 – 2.83 Å.

Recently, the chemical bonding situation of LiAuSn (planar Au_3Sn_3 nets) and $LiAu_3Sn_4$ (NiAs type related trigonal tin centred gold prisms) was reported [41] showing strong Au-Sn interactions at distances of d(Au-Sn) = 2.70 Å for LiAuSn and d(Au-Sn) = 2.69 – 3.02 Å for $LiAu_3Sn_4$. Au-Au bond distances present in $LiAu_3Sn_4$ are of the same range (d(Au-Au) = 2.85 Å) as observed for the Au_3Sn heteroclusters in Au_3SnP_7. While the previously mentioned systems are mainly metallic in character, in this context one should also discuss organometallic compounds, featuring AuSn heteroclusters bonded to ligands in a more covalent way. Illustrative examples are Au_2Sn_2 clusters realised for the stannaborate adducts with gold electrophiles

Table 5. Selected bond distances [Å] for Au_3SnCuP_{10} and Au_3SnP_7.

Au_3SnCuP_{10} refinement 1		
Cu1-P1	2.310(4)	4×
Au2-Sn2	0.314(17)	
Au2-Sn2	2.774(17)	3×
Au2-P2	2.443(6)	3×
Sn2-Sn2	2.51(2)	3×
Sn2-P2	2.601(17)	3×
P1-P2	2.193(6)	3×
Au_3SnCuP_{10} refinement 2		
Cu1/Au1-P1	2.303(4)	4×
M2-M2	2.935(2)	4×
M2-P2	2.470(4)	3×
P1-P2	2.193(7)	3×
Au_3SnP_7 crystal 1		
Au1-Au2	2.864(1)	2×
Au1-Sn	2.705(1)	
Au1-P2	2.410(4)	2×
Au1-P4	2.421(6)	
Au2-Sn	2.768(2)	
Au2-P1	2.471(5)	
Au2-P2	2.388(3)	
Au2-P3	2.382(4)	
Sn-P3	2.573(5)	2×
Sn-P4	2.588(5)	
P1-P2	2.184(6)	
P1-P3	2.157(5)	
P1-P4	2.171(6)	
P2-P3	2.170(6)	
Au_3SnP_7 crystal 2		
Au1a/Sn1a-Au2	2.884(1)	2×
Au1a/Sn1a-Au1b/Sn1b	2.777(1)	2×
Au1a/Sn1a-P2	2.496(4)	2×
Au1a/Sn1a-P4	2.502(5)	
Au2-Au1b/Sn1b	2.856(1)	2×
Au2-P1	2.502(4)	
Au2-P2	2.419(3)	
Au2-P3	2.412(4)	
Au1b/Sn1b-P	2.542(4)	2×
Au1b/Sn1b-P4	2.552(5)	
P1-P2	2.195(6)	
P1-P3	2.197(5)	
P1-P4	2.200(5)	
P2-P3	2.184(5)	

like $[Bu_3NH]_2[(Ph_3P)Au(SnB_{11}H_{11})]_2$ [42] and related compounds [43]. Those systems can be regarded as model compounds for the covalent $[Au_3Sn]$ cluster – $^1_\infty[P_7]$ polyphosphide interactions expected for the present material and found for the M_3Sn cluster in Cu_3SnCuP_{10} and Ag_3SnP_7. Distances of d(Au-Au) = 2.60–2.89 Å and d(Au-Sn) = 2.71–3.12 Å were reported for the stannaborate systems. One has to separate two different cases of Au-Au interactions in Au-Sn cluster chemistry, depending on the bonding situation of a certain gold atom. Au-Au bond distances in the $[Au_8(PPh_3)_7SnCl_3]^+$ cation of $[Au_8(PPh_3)_7SnCl_3]_2[SnCl_6]$ [44] vary from 2.63–2.68 Å for a pure gold environment (only gold as next neighbours) and from 2.84–2.97 Å if gold is also bonded either to tin or to phosphorus. The second case is realized for the Au_3Sn heteroclusters in Au_3SnP_7 where the cluster is coordinated by the $^1_\infty[P_7]$ polyphosphide (see Fig. 5) to form three M-P- in addition to three M-M bonds per cluster atom. The observed Au-Au distance in Au_3SnP_7 of d(Au-Au) = 2.864(1) Å perfectly fits the second case.

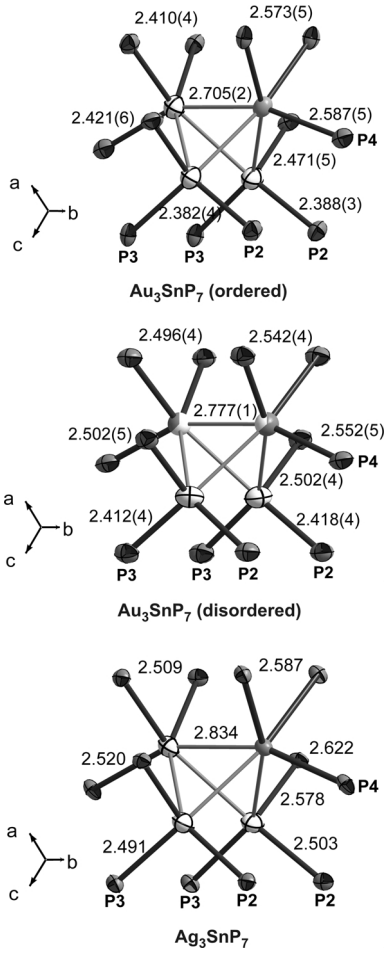

Fig. 5. M/Sn-P bond distance distribution observed for the first coordination sphere of the M_3Sn heteroclusters in Au_3SnP_7 and Ag_3SnP_7 [16]. Bond distances for Au-P, Ag-P and mixed Au/Sn-P are clearly separated from each other.

The $^1_\infty[P_7]$ polyphosphide unit is built up of six-membered phosphorus rings in chair conformation linked by a two-bonded P-atom in 1,4-position. A P-P bond distance range from 2.157(5) to 2.184(6) Å

was observed slightly smaller than in Ag_3SnP_7 (2.18–2.20 Å). Bond distances in polyphosphides vary over a wide range from 2.15 to 2.30 Å and are dependent on structural parameters, the relative charges of the P atoms and different strain in the arrangements [3]. Postulating a purely ionic representation of the heterocluster and the polyphosphide unit the cluster carries the formal charge 5+ and the polyphosphide unit 5−, in accordance with the number of three- and two-bonded P atoms (*c.f.* Fig. 4). An electron count of 0.71 electrons per P atom results certainly reduced by the limited charge transfer due to the predominantly covalent bond interaction. NdP_5 [45], a polyphosphide with ${}^{2}_{\infty}[P_5]^{3-}$ units and a formal charge of 0.6 electrons per P atom, shows a similar P-P distance dispersion of 2.16 to 2.21 Å. The influence of the strain can easily be seen on comparing the bond distances of $MoFe_2P_{12}$ [46] with ${}^{1}_{\infty}[P_6]^{4-}$ chains of six-membered P rings in boat conformation. A formal charge of 0.5 electrons per atom is leading to a certain stretching of the bonds to $d(\text{P-P}) = 2.24-2.27$ Å.

Going from the ordered to the disordered form of Au_3SnP_7 the situation does not change in principle. All bond distances are slightly increased for the cluster as well as for the polyphosphide units. The bond distance distribution of the cluster atoms to the polyphosphide atoms is a good indicator for the degree of disorder on the mixed occupied 2*e* cluster positions. Sn-P distances vary between 2.573(5) and 2.587(5) Å while Au-P distances are between 2.382(4) and 2.471(5) Å (Fig. 5). Dependent on the Sn occupancy realised on the mixed occupied 2*e* positions, the distances to the polyphosphide units are around 2.55 Å for the high tin content and around 2.50 Å for the low one.

Conclusion

Au_3SnCuP_{10} and Au_3SnP_7 close a gap in M_3Sn heterocluster chemistry with the formation of formerly unseen Au_3Sn and $Au_{3-x}Cu_xSn$ heteroclusters. The heteroclusters are embedded between adamantane type P_{10} cages and ${}^{1}_{\infty}[P_7]$ units previously observed only for isostructural M_3SnCuP_{10} and Ag_3SnP_7. The structures of both gold tin polyphosphides are characterized by different types of disorder localized within the cation substructures. Tin (IV) iodide was used as mineralization promoter in conventional solid state reactions from elemental starting materials to increase the overall yields of the polyphosphides in relation to binary side products.

Experimental Section

Preparation

SnI_4 was prepared by refluxing a mixture of tin (12 g, Heraeus, 99.999%) and iodine (40 g, Chempur, resublimated) in 250 ml of toluene for ≈ 30 min until the violet colour of iodine disappeared. After decanting the hot solution from the remaining tin, orange SnI_4 crystallized after cooling to r. t. The crude product was recrystallized from toluene [47].

Au_3SnCuP_{10} was prepared from a 3 : 1 : 1 : 10 mixture of gold (0.4035 g, Chempur, 99.999%), tin (0.0810 g, Heraeus, 99.999%), copper (0.0434 g, Chempur, 99.999%) and red phosphorus (0.2115 g, Chempur, 99.999+%). The starting materials were sealed into an evacuated silica tube and annealed at 820 K for one week. The crude product was homogenized by grinding, resealed and further annealed at 820 K for two weeks. This process was repeated three times within an overall annealing time of six weeks.

Au_3SnP_7 was prepared from a 3 : 1 : 7 mixture of gold (0.6175 g, Chempur, 99.999%), tin (0.1240 g, Heraeus, 99.999%) and red phosphorus (0.2266 g, Chempur, 99.999+%). A small amount of SnI_4 (20 mg) was added as a mineralization agent. The starting materials were sealed into an evacuated silica tube and annealed at 820 K for eleven days, followed by slow cooling at the rate of 50 K/min to r.t. After homogenization by grinding the product was resealed into an ampoule and further annealed at 820 K for two more weeks. Even after prolonged annealing periods Au_3SnP_7 was always accompanied by small amounts of Au_2P_3 and gold tin intermetallic compounds. Single crystals suitable for X-ray structure determination were isolated from the bulk phase. Preparations directly from the elements without SnI_4 led to an increase of binary phases and the formation of white phosphorus.

Semiquantitative EDX analyses

Electronmicroscopic measurements were performed using a Leica 420i scanning electron microscope (Zeiss) fitted with an electron dispersive detector unit (Oxford). Cu, Ag, Sn, GaP were used as standards for calibration. A voltage of 20 kV was applied to the samples. All single crystals used for structure determinations and additional crystals separated form the reaction batches were analyzed. Crystals were prepared on graphite tape and mounted on aluminium carriers prior to the analyses. Three to five independent analyses were averaged for each compound. The results are summarized in Table 1.

X-ray powder and single crystal diffraction

X-ray powder phase analytical investigations were carried out for both compounds. Finely ground samples were fixed on an X-ray transparent foil and measured in transmission geometry applying Cu-$K_{\alpha 1}$ radiation (germanium

monochromator, $\lambda = 1.54051$ Å). Data were collected at 293 K from 10 to 80° 2θ using a Stoe StadiP powder diffractometer equipped with a linear 5° PSD (Brown). Si was used as external standard.

Single crystals suitable for X-ray structure determination were isolated from the reaction batches. Intensity data for both compounds were collected on an Enraf-Nonius CAD4 (Au_3SnCuP_{10}) or a Stoe IPDS II (Au_3SnP_7) single crystal diffractometer both operated with Mo-K_α radiation ($\lambda = 0.71073$ Å). After a correction of Lorentz, polarisation and absorption effects the structures were solved by direct methods using the Shelxs program [48]. Absorption corrections were performed prior to all structure refinements based on optimized crystal shapes from symmetry equivalent reflections using the programs X-shape and Xred [49]. Refinements were performed with the program package JANA2000 [50]. Further details of the crystal structure investigations are available from the Fachinformationszentrum Karlsruhe, D-76344 Eggenstein-Leopoldshafen (Germany) on quoting the depository numbers CSD-416406 (Au_3SnCuP_{10}, refinement 2), CSD-416407 (Au_3SnP_7, crystal 1) and CSD-416408 (Au_3SnP_7, crystal 2) , the name of the author and citation of the paper.

Acknowledgement

The preparation of semiquantitative EDX measurements by H. J. Göcke is gratefully acknowledged.

[1] A. Pfitzner, Angew. Chem. Int. Ed. **45**, 699 (2006) and references herein.
[2] H. G. von Schnering, Chem. Rev. **88**, 243 (1988), and references herein.
[3] R. Pöttgen, W. Hönle, H. G. von Schnering, in R. B. King (ed.): Encyclopedia of Inorganic Chemistry, 2nd Ed., Vol. VII, p. 4255, Wiley, Chichester (2005) and references herein.
[4] M. G. Kanatzidis, R. Pöttgen, W. Jeitschko, Angew. Chem. **117**, 7156 (2005).
[5] M. Baudler, D. Düster, K. Langerbeins, J. Germeshausen, Angew. Chem. **96**, 309 (1984).
[6] M.-P. Bichat, J.-L. Pascal, F. Gillot, F. Favier, Chem. Mater. **17**, 6761 (2005).
[7] M.-P. Bichat, T. Politova, J. L. Pascal, F. Favier, L. Monconduit, J. Electrochem. Soc. **151**, A2074 (2004).
[8] H. Schlenger, H. Jakobs, R. Juza, Z. Anorg. Allg. Chem. **385**, 177 (1971).
[9] O. Olofsson, Acta Chem. Scand. **19**, 229 (1965).
[10] M. H. Möller, W. Jeitschko, Z. Anorg. Allg. Chem. **491**, 225 (1982).
[11] M. H. Möller, W. Jeitschko, Inorg. Chem. **20**, 828 (1981).
[12] H. Schlenger, H. Jacobs, Acta Crystallogr. B **28**, 327 (1972).
[13] H. Schlenger, H. Jacobs, R. Juza, Z. Anorg. Allg. Chem. **385**, 177 (1971).
[14] W. Hönle, H. G. von Schnering, Z. Kristallogr. **153**, 339 (1980).
[15] N. A. Goryunova, V. M. Orlov, V. I. Sokolova, G. P. Shepenkov, E. V. Tsvetkova, Phys. Stat. Sol. A **3**, 75 (1970).
[16] M. M. Shatruk, K. A. Kovnir, A. V. Shevelkov, B. A. Popovkin, Angew. Chem. **112**, 2561 (2000); Angew. Chem. Int. Ed. **39**, 2508 (2000).
[17] S. Lange, C. P. Sebastian, L. Zhang, H. Eckert, T. Nilges, Inorg. Chem. (2006), in press.
[18] D. W. Bullet, W. G. Dawson, Solid State Commun. **60**, 767 (1986).
[19] W. Jeitschko, M. H. Möller, Acta Crystallogr. B **35**, 573 (1979).
[20] M. M. Shatruk, K. A. Kovnir, A. V. Shevelkov, I. A. Presniakov, B. A. Popovkin, Inorg. Chem. **38**, 3455 (1999).
[21] O. Olofsson, Acta Chem. Scand. **21**, 1659 (1967).
[22] L. Pauling, J. Am. Chem. Soc. **69**, 542 (1947).
[23] A. Bayler, A. Schier, G. A. Bowmaker, H. Schmidbaur, J. Am. Chem. Soc. **118**, 7006 (1996).
[24] P. Pyykkö, Angew. Chem. Int. Ed. **43**, 4412 (2004).
[25] P. Pyykkö, Inorg. Chim. Acta **358**, 4113 (2005).
[26] U. D. Scholz, W. Jeitschko, J. Solid State Chem. **67**, 271 (1987).
[27] M. Eschen, J. Wallinda, W. Jeitschko, Z. Anorg. Allg. Chem. **628**, 2764 (2002).
[28] G. A. Bowmaker, B. J. Kennedy, J. C. Reid, Inorg. Chem. **37**, 3968 (1998).
[29] B. Standke, M. Jansen, Z. Anorg. Allg. Chem. **535**, 39 (1986).
[30] P. G. Jones, H. Rumpel, E. Schwarzmann, G. M. Sheldrick, Acta Crystallogr. **35b**, 1435 (1979).
[31] J. K. Brandon, R. Brezard, W. B. Pearson, D. J. N. Tozer, Acta Crystallogr. **33b**, 527 (1977).
[32] T. Heumann, N. Harmsen, Z. Metallkd. **61**, 906 (1970).
[33] M. Feller-Kniepmeier, T. Heumann, Z. Metallkd. **51**, 404 (1960).
[34] N. Korber, J. Daniels, Helv. Chim. Acta **79**, 2083 (1996).
[35] D. Knettel, M. Reil, N. Korber, Z. Naturforsch. **56b**, 965 (2001).
[36] K. Schubert, U. Rösler, Z. Metallkd. **41**, 298 (1950).
[37] H. D. Sinnen, H. U. Schuster, Z. Naturforsch. **36b**, 833 (1981).

[38] H. D. Sinnen, H. U. Schuster, Z. Naturforsch. **33b**, 1077 (1978).
[39] U. Ch. Rodewald, R.-D. Hoffmann, Z. Wu, R. Pöttgen, Z. Naturforsch. **61b**, 108 (2006).
[40] S. Lange, T. Nilges, R.-D. Hoffmann, R. Pöttgen, Z. Anorg. Allg. Chem. **632**, 1163 (2006).
[41] R.-D. Hoffmann, D. Johrendt, Z. Wu, R. Pöttgen, J. Mater. Chem. **12**, 676 (2002).
[42] S. Hagen, I. Pantenburg, F. Weigend, C. Wickleder, L. Wesemann, Angew. Chem. Int. Ed. **42**, 1501 (2003).
[43] S. Hagen, L. Wesemann, I. Pantenburg, Chem. Commun. 1013 (2005).
[44] Z. Demidowicz, R. L. Johnston, J. C. Machell, D. M. Mingos, I. D. Williams, J. Chem. Soc. Dalton Trans. 1751 (1988).
[45] W. Wichelhaus, H. G. von Schnering, Z. Anorg. Allg. Chem. **419**, 77 (1976).
[46] U. Flörke, W. Jeitschko, Inorg. Chem. **22**, 1736 (1983).
[47] G. Brauer, Handbuch der Präparativen Anorganischen Chemie, 3rd. ed., Vol. 2, p. 759, F. Enke, Stuttgart (1978).
[48] G. M. Sheldrick, SHELXS-97, Program for Crystal Structure Refinement, University of Göttingen, Germany (1997). [49] Xred Ver. 1.10 and Xshape Ver. 2.05 program packages, Stoe & Cie GmbH, Darmstadt (2005).
[49] V. Petricek, M. Dusek, L. Palatinus, Jana2000 – The crystallographic computing system, Institute of Physics, Prague, Czech Republic (2000).